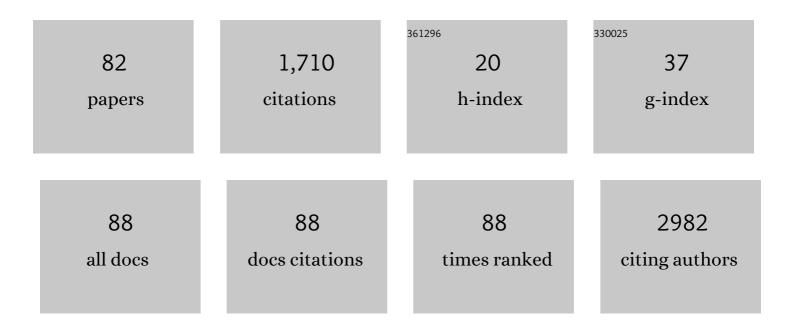
## Vincent Dunet

List of Publications by Year in descending order

Source: https://exaly.com/author-pdf/7132040/publications.pdf Version: 2024-02-01



#	Article	IF	CITATIONS
1	ASPECTS-based selection for late endovascular treatment: a retrospective two-site cohort study. International Journal of Stroke, 2022, 17, 434-443.	2.9	6
2	MRI software for diffusion-perfusion mismatch analysis may impact on patients' selection and clinical outcome. European Radiology, 2022, 32, 1144-1153.	2.3	9
3	Patterns of ischemic posterior circulation strokes: A clinical, anatomical, and radiological review. International Journal of Stroke, 2022, 17, 714-722.	2.9	28
4	Intravenous rtPA Before Thrombectomy Versus Thrombectomy Alone in Strokes With Unknown Time of Onset. Stroke, 2022, , STROKEAHA121037741.	1.0	0
5	Radiological evolution of autograft fat used for skull base reconstruction after transsphenoidal surgery for pituitary adenomas. Pituitary, 2022, 25, 468-473.	1.6	7
6	Overview of the RGD-Based PET Agents Use in Patients With Cardiovascular Diseases: A Systematic Review. Frontiers in Medicine, 2022, 9, .	1.2	5
7	<scp>Magnetic Resonance Imaging</scp> or <scp>Computed Tomography</scp> for Suspected Acute Stroke: Association of Admission Image Modality with Acute Recanalization Therapies, Workflow Metrics, and Outcomes. Annals of Neurology, 2022, 92, 184-194.	2.8	6
8	A Fetal Brain magnetic resonance Acquisition Numerical phantom (FaBiAN). Scientific Reports, 2022, 12,	1.6	4
9	Pattern of cognitive deficits in severe COVID-19. Journal of Neurology, Neurosurgery and Psychiatry, 2021, 92, 567-568.	0.9	108
10	Early discrimination of cognitive motor dissociation from disorders of consciousness: pitfalls and clues. Journal of Neurology, 2021, 268, 178-188.	1.8	19
11	Prediction of tumour grade and survival outcome using pre-treatment PET- and MRI-derived imaging features in patients with resectable pancreatic ductal adenocarcinoma. European Radiology, 2021, 31, 992-1001.	2.3	9
12	Discriminating cognitive motor dissociation from disorders of consciousness using structural MRI. NeuroImage: Clinical, 2021, 30, 102651.	1.4	6
13	Correlation between ASPECTS and Core Volume on CT Perfusion: Impact of Time since Stroke Onset and Presence of Large-Vessel Occlusion. American Journal of Neuroradiology, 2021, 42, 422-428.	1.2	32
14	Simulated Half-Fourier Acquisitions Single-shot Turbo Spin Echo (HASTE) ofÂthe Fetal Brain: Application toÂSuper-Resolution Reconstruction. Lecture Notes in Computer Science, 2021, , 157-167.	1.0	0
15	Differentiation between benign and malignant vertebral compression fractures using qualitative and quantitative analysis of a single fast spin echo T2-weighted Dixon sequence. European Radiology, 2021, 31, 9418-9427.	2.3	13
16	Discussing Challenges in Diagnosis of Tuberculous Meningitis and Neurosarcoidosis. Canadian Journal of Neurological Sciences, 2021, , 1-7.	0.3	0
17	Broadening INPP5E phenotypic spectrum: detection of rare variants in syndromic and non-syndromic IRD. Npj Genomic Medicine, 2021, 6, 53.	1.7	8
18	Fetal Brain Biometric Measurements on 3D Super-Resolution Reconstructed T2-Weighted MRI: An Intra- and Inter-observer Agreement Study. Frontiers in Pediatrics, 2021, 9, 639746.	0.9	13

#	Article	IF	CITATIONS
19	Imaging angiogenesis in atherosclerosis in large arteries with 68Ga-NODAGA-RGD PET/CT: relationship with clinical atherosclerotic cardiovascular disease. EJNMMI Research, 2021, 11, 71.	1.1	12
20	Predictive Patterns of Glutamine Synthetase Immunohistochemical Staining in CTNNB1-mutated Hepatocellular Adenomas. American Journal of Surgical Pathology, 2021, 45, 477-487.	2.1	28
21	Negative 18F-FET PET/CT in brain metastasis recurrence: a teaching case report. European Journal of Hybrid Imaging, 2021, 5, 21.	0.6	0
22	Pulmonary Lymphangitic Carcinomatosis: Diagnostic Performance of High-Resolution CT and <sup>18</sup> F-FDG PET/CT in Correlation with Clinical Pathologic Outcome. Journal of Nuclear Medicine, 2020, 61, 26-32.	2.8	14
23	Pulmonary embolism during pregnancy: a 17-year single-center retrospective MDCT pulmonary angiography study. European Radiology, 2020, 30, 1780-1789.	2.3	8
24	Thrombectomy and Thrombolysis of Isolated Posterior Cerebral Artery Occlusion. Stroke, 2020, 51, 254-261.	1.0	83
25	Eligibility for late endovascular treatment using DAWN, DEFUSE-3, and more liberal selection criteria in a stroke center. Journal of NeuroInterventional Surgery, 2020, 12, 842-847.	2.0	28
26	Lung MRI assessment with high-frequency noninvasive ventilation at 3â€⁻T. Magnetic Resonance Imaging, 2020, 74, 64-73.	1.0	8
27	Impact of CT venography added to CT pulmonary angiography for the detection of deep venous thrombosis and relevant incidental CT findings. European Journal of Radiology, 2020, 133, 109388.	1.2	3
28	Progressive multifocal leukoencephalopathy responsive to withdrawal of imatinib in a patient with FIP1L1-PDGFRA positive myeloid neoplasm. Leukemia and Lymphoma, 2020, 61, 2226-2229.	0.6	1
29	MRI–EEG correlation for outcome prediction in postanoxic myoclonus. Neurology, 2020, 95, e335-e341.	1.5	20
30	Automated MRI-based volumetry of basal ganglia and thalamus at the chronic phase of cortical stroke. Neuroradiology, 2020, 62, 1371-1380.	1.1	10
31	Feeding artery aneurysms associated with large meningiomas: case report and review of the literature. Heliyon, 2020, 6, e04071.	1.4	6
32	ANCA-associated life-threatening systemic vasculitis after alemtuzumab treatment for multiple sclerosis. Multiple Sclerosis Journal, 2020, 26, 1599-1602.	1.4	8
33	Head and neck tumors angiogenesis imaging with 68Ga-NODAGA-RGD in comparison to 18F-FDG PET/CT: a pilot study. EJNMMI Research, 2020, 10, 47.	1.1	21
34	Episodic memory decline in Parkinson' s disease: relation with white matter hyperintense lesions and influence of quantification method. Brain Imaging and Behavior, 2019, 13, 810-818.	1.1	20
35	Collaterals are a major determinant of the core but not the penumbra volume in acute ischemic stroke. Neuroradiology, 2019, 61, 971-978.	1.1	27
36	Otogenic Pneumocephalus Presenting as Pneumatocele of the Scalp. American Journal of Medicine, 2019, 132, 1170-1172.	0.6	1

#	Article	IF	CITATIONS
37	Ultrashort echo time imaging of the lungs under highâ€frequency noninvasive ventilation: A new approach to lung imaging. Journal of Magnetic Resonance Imaging, 2019, 50, 1789-1797.	1.9	10
38	MR Volumetry of Lung Nodules: A Pilot Study. Frontiers in Medicine, 2019, 6, 18.	1.2	6
39	Diagnosis and treatment of invasive fungal infections: looking ahead. Journal of Antimicrobial Chemotherapy, 2019, 74, ii27-ii37.	1.3	66
40	Focal Hypoperfusion in Acute Ischemic Stroke Perfusion CT: Clinical and Radiologic Predictors and Accuracy for Infarct Prediction. American Journal of Neuroradiology, 2019, 40, 483-489.	1.2	8
41	A blackâ€blood ultraâ€short echo time (UTE) sequence for 3D isotropic resolution imaging of the lungs. Magnetic Resonance in Medicine, 2019, 81, 3808-3818.	1.9	6
42	Optimizing radiation dose parameters in MDCT arthrography of the shoulder: illustration of basic concepts in a cadaveric study. Skeletal Radiology, 2019, 48, 1261-1268.	1.2	3
43	Response of locally advanced rectal cancer (LARC) to radiochemotherapy: DW-MRI and multiparametric PET/CT in correlation with histopathology. Nuklearmedizin - NuclearMedicine, 2019, 58, 28-38.	0.3	16
44	Multiple nivolumab-induced CNS demyelination with spontaneous resolution in an asymptomatic metastatic melanoma patient. , 2019, 7, 336.		21
45	Practical clinical guidelines for contouring the trigeminal nerve (V) and its branches in head and neck cancers. Radiotherapy and Oncology, 2019, 131, 192-201.	0.3	19
46	Impact of model-based iterative reconstruction (MBIR) on image quality in cerebral CT angiography before and after intracranial aneurysm treatment. European Journal of Radiology, 2018, 102, 109-114.	1.2	7
47	Bone Marrow Metastases: T2-weighted Dixon Spin-Echo Fat Images Can Replace T1-weighted Spin-Echo Images. Radiology, 2018, 286, 948-959.	3.6	82
48	Late Lyme neuroborreliosis with chronic encephalomyelitis. Neurology, 2018, 91, 627-628.	1.5	6
49	Letter to the Editor. Surgery for pediatric thalamic tumors: using DTI to improve neurological outcome. Journal of Neurosurgery: Pediatrics, 2018, 22, 716-718.	0.8	0
50	Voxel-based 18F-FET PET segmentation and automatic clustering of tumor voxels: A significant association with IDH1 mutation status and survival in patients with gliomas. PLoS ONE, 2018, 13, e0199379.	1.1	19
51	Republished: Renal cell carcinoma metastasis involving vertebral hemangioma: dual percutaneous treatment by navigational bipolar radiofrequency ablation and high viscosity cement vertebroplasty. Journal of NeuroInterventional Surgery, 2017, 9, e34-e34.	2.0	6
52	Detection and Viability of Colorectal Liver Metastases After Neoadjuvant Chemotherapy. Clinical Nuclear Medicine, 2017, 42, 258-263.	0.7	12
53	Impact of metal artifact reduction software on image quality of gemstone spectral imaging dual-energy cerebral CT angiography after intracranial aneurysm clipping. Neuroradiology, 2017, 59, 845-852.	1.1	29
54	Performance of highly sensitive cardiac troponin T assay to detect ischaemia at PET-CT in low-risk patients with acute coronary syndrome: a prospective observational study. BMJ Open, 2017, 7, e014655.	0.8	6

#	Article	IF	CITATIONS
55	First in-human radiation dosimetry of 68Ga-NODAGA-RGDyK. EJNMMI Research, 2017, 7, 43.	1.1	24
56	MRI volumetric morphometry in vascular parkinsonism. Journal of Neurology, 2017, 264, 1511-1519.	1.8	8
57	Liver and biliary damages following transarterial chemoembolization of hepatocellular carcinoma: comparison between drug-eluting beads and lipiodol emulsion. European Radiology, 2017, 27, 1431-1439.	2.3	83
58	Intradural lumbar disc herniation detected by 3D CISS MRI. BMJ Case Reports, 2017, 2017, bcr-2017-221728.	0.2	9
59	Renal cell carcinoma metastasis involving vertebral hemangioma: dual percutaneous treatment by navigational bipolar radiofrequency ablation and high viscosity cement vertebroplasty. BMJ Case Reports, 2017, 2017, bcr2016012931.	0.2	2
60	Incidental extracardiac findings on cardiac MR: Systematic review and meta-analysis. Journal of Magnetic Resonance Imaging, 2016, 43, 929-939.	1.9	24
61	Initial Staging of Locally Advanced Rectal Cancer and Regional Lymph Nodes. Clinical Nuclear Medicine, 2016, 41, 289-295.	0.7	21
62	CT imaging in pre-therapeutic assessment of lung cancer. Diagnostic and Interventional Imaging, 2016, 97, 973-989.	1.8	9
63	Cognitive Impairment and Basal Ganglia Functional Connectivity in Vascular Parkinsonism. American Journal of Neuroradiology, 2016, 37, 2310-2316.	1.2	15
64	Effects of continuous positive airway pressure treatment on coronary vasoreactivity measured by 82Rb cardiac PET/CT in obstructive sleep apnea patients. Sleep and Breathing, 2016, 20, 673-679.	0.9	1
65	Glioblastoma Multiforme Recurrence. Radiology, 2016, 280, 326-327.	3.6	Ο
66	Response to: Performance of <sup>18</sup> F-FET-PET versus <sup>18</sup> F-FDG-PET for the diagnosis and grading of brain tumors: inherent bias in meta-analysis not revealed by quality metrics. Neuro-Oncology, 2016, 18, 1029-1030.	0.6	4
67	Current artefacts in cardiac and chest magnetic resonance imaging: tips and tricks. British Journal of Radiology, 2016, 89, 20150987.	1.0	17
68	Focal pleural thickening mimicking pleural plaques on chest computed tomography: tips and tricks. British Journal of Radiology, 2016, 89, 20150792.	1.0	22
69	Thoracic fat volume is independently associated with coronary vasomotion. European Journal of Nuclear Medicine and Molecular Imaging, 2016, 43, 280-287.	3.3	0
70	Myocardial blood flow quantification by Rb-82 cardiac PET/CT: A detailed reproducibility study between two semi-automatic analysis programs. Journal of Nuclear Cardiology, 2016, 23, 499-510.	1.4	29
71	Chest CT at a dose below 0.3 mSv: impact of iterative reconstruction on image quality and lung analysis. Acta Radiologica, 2016, 57, 311-317.	0.5	6
72	Performance of <sup>18</sup> F-FET versus <sup>18</sup> F-FDG-PET for the diagnosis and grading of brain tumors: systematic review and meta-analysis. Neuro-Oncology, 2016, 18, 426-434.	0.6	143

#	Article	IF	CITATIONS
73	Impact of Extracardiac Findings during Cardiac MR on Patient Management and Outcome. Medical Science Monitor, 2015, 21, 1288-1296.	0.5	10
74	Diagnostic accuracy of F-18-fluoroethyltyrosine PET and PET/CT in patients with brain tumor. Clinical and Translational Imaging, 2013, 1, 135-144.	1.1	3
75	FET PET in Neuro-oncology and in Evaluation of Treatment Response. PET Clinics, 2013, 8, 147-162.	1.5	8
76	Added prognostic value of myocardial blood flow quantitation in rubidium-82 positron emission tomography imaging. European Heart Journal Cardiovascular Imaging, 2013, 14, 1203-1210.	0.5	96
77	Diffusion-weighted magnetic resonance imaging in metastatic gastrointestinal stromal tumor (GIST): a pilot study on the assessment of treatment response in comparison with 18F-FDG PET/CT. Acta Radiologica, 2013, 54, 837-842.	0.5	20
78	Multiple pulmonary artery aneurysms in tuberous sclerosis complex. BMJ Case Reports, 2013, 2013, bcr2012007911.	0.2	9
79	Assessment of Coronary Vasoreactivity by Multidetector Computed Tomography - Feasibility Study With Rubidium-82 Cardiac Positron Emission Tomography Circulation Journal, 2012, 76, 160-167.	0.7	6
80	Performance of <sup>18</sup> F-Fluoro-Ethyl-Tyrosine ( <sup>18</sup> F-FET) PET for the Differential Diagnosis of Primary Brain Tumor: A Systematic Review and Metaanalysis. Journal of Nuclear Medicine, 2012, 53, 207-214.	2.8	222
81	Voriconazole-induced periostitis. European Journal of Nuclear Medicine and Molecular Imaging, 2012, 39, 375-376.	3.3	21
82	Effects of paraoxonase activity and gene polymorphism on coronary vasomotion. EJNMMI Research, 2011, 1, 27.	1.1	4